Vision Research: Ms. No. VR-19-327 REVISION

7th May 2020

The electrophysiological response to polarization-modulated patterned visual stimuli

Stephen J. Anderson[1,2]
Andrea Edson-Scott[2]
& *Gary P. Misson[1,3]

[1]School of Life & Health Sciences, Aston University, Birmingham, B4 7ET, UK

[2]Aston Neuroscience Institute, Aston University, Birmingham, B4 7ET, UK

[3]Dept of Ophthalmology, South Warwickshire NHS Foundation Trust, Lakin Road, Warwick, CV34 5BW, UK

***Correspondence to**: Prof. Gary P Misson at g.misson@aston.ac.uk

Key words:

- macular disease
- polarized light
- human vision
- primate vision
- visual evoked cortical potentials
- pattern electroretinogram

Abstract

Recent reports indicate that the subjective ability of humans to discriminate between polarisation **E**-vector orientations approaches that of many invertebrates. Here, we show that polarisation-modulated patterned stimuli generate an objectively recordable electrophysiological response in humans with normal vision. We investigated visual evoked potential (VEP) and electroretinographic (ERG) responses to checkerboard patterns defined solely by their polarisation **E**-vector orientation alternating between ±45°. Correcting for multiple comparisons, paired-samples t-tests were conducted to assess the significance of post-stimulus deflections from baseline measures of noise. Using standard check pattern sizes for clinical electrophysiology, and a pattern-reversal protocol, participants showed a VEP response to polarization-modulated patterns (PolVEP) with a prominent and consistent positive component near 150 ms ($p < 0.01$), followed by more variable negative components near 200 ms and 300 ms. The effect was unrecordable with visible wavelengths greater than 550 nm. Further, pseudo-depolarisation negated the responses, while control studies provided confirmatory evidence that the PolVEP response was not the product of luminance artefacts. Polarization-modulated patterns did not elicit a recordable ERG response. The possible origins of the PolVEP signals, and the absence of recordable ERG signals, are discussed. We conclude that evoked cortical responses to polarization-modulated patterns provide an objective measure of foveal function, suitable for both humans and non-human primates with equivalent macular anatomy.

1. Introduction

Sensitivity to light polarization is widespread and well developed in invertebrates, where it is sufficiently advanced to be termed polarization vision. It is rudimentary and of questionable physiological significance in non-aquatic vertebrates, although polarization sensitivity is likely in some fish (reviewed in Horváth, 2014). In humans, it has long been believed that polarization sensitivity is limited to the perception of Haidinger's brushes, a vague and fleeting entoptic phenomenon generated by viewing a uniformly linear polarized field (McGregor, Temple & Horváth, 2014). However, recent psychophysical findings have demonstrated that human polarization perception is more acute and well developed than previously thought (Misson, Timmerman & Bryanston-Cross, 2015; Temple, McGregor, Miles, Graham, Miller, Buck, Scott-Samuel & Roberts, 2015). For example, stimuli comprising sharp-edged patterned zones modulated by angle of linear polarization are perceived in humans with a resolution as low as 4.4° difference in angle of polarization across the discontinuous boundary (Misson and Anderson, 2017; see also Misson et al., 2019). This visual attribute has been termed polarization pattern perception (Misson and Anderson, 2017).

As with Haidinger's brushes, polarization pattern perception (PPP) results from differential absorption of linear polarized light by radially symmetric diattenuating structures within the fovea of the central macula (Misson, Temple & Anderson, 2019), and correlates with the distribution and density of macular pigment and the radial architecture of the Henle fibre layer (Misson & Anderson, 2017). The foveal origin of both phenomena implies that any electrophysiological response to a polarization stimulus is specifically dependent on the structural and functional integrity of the fovea and foveal visual pathways. This specificity led to propositions that Haidinger's brushes and PPP might be clinically useful, particularly with respect to the early diagnosis and management of age-related macular degeneration (Goldschmidt, 1950; Muller, Muller, Gliem, Kupper, Holz, Harmening & Charbel Issa, 2016; Stanworth & Naylor, 1955; Temple, Roberts & Misson, 2019).

While an objective electrophysiological response to the onset/offset of Haidinger's brushes has been reported (Dodt & Kuba, 1990; Dodt, Tsuyama & Kuba, 1994), an objective measure of PPP, which is arguably a more salient and quantifiable stimulus than Haidinger's brushes, has not been attempted. Our aim in this study was to assess cortical evoked potential and electroretinographic responses to patterned polarization stimuli, responses that must be purely macular in origin.

2. Methods

There were two main experiments. In **Experiment 1**, a series of VEP control measures were conducted to establish that a polarization-dependent response existed and that our protocol for assessing polarization responses did not produce any confounding luminance artefacts in the stimulus display. In **Experiment 2**, we assessed both VEP and pattern electroretinographic (PERG) responses to stimuli defined solely by their polarisation **E**-vector orientation.

2.1 Stimulus generation and calibration

Standard checkerboard patterns were generated by a Micromed Pattern 10 device (Micromed, Mogliano Veneto, Italy). An isoluminant, isochromatic polarization pattern was achieved by displaying the generated stimuli on a conventional LED-backlit thin-film transistor liquid crystal display (TFT LCD) from which the front polarizing filter had been removed (i.e. delaminated) (Foster, Temple, How, Daly, Sharkey, Wilby & Roberts, 2018; Misson et al., 2015; Temple et al., 2015).

In Experiment 1 (preliminary and control studies), the display screen was a delaminated 7-inch 800 x 480 pixels TFT LCD (from Waveshare Electronics, Shenzhen, China), with an exchangeable filter tray serving in place of the front polarizer. This small screen was used for practical considerations, because it was necessary to mask the entire screen with one of several filters. The characteristics of the various filters employed, and the rationale for their use, are given in Table 1. The angular dimensions of this screen at a viewing distance of 0.25m were 19.8° (w) x 18.2° (h).

In Experiment 2 (main polarization studies), the display screen was a delaminated 27-inch 1920 x 1080 pixels TFT LCD (Asus VS278H screen, from ASUSTeK Computer Inc, Taiwan). A blue filter ('B', from Table 1) with a peak transmission of 440 – 460 nm, matching the absorption spectrum of macular pigment, was placed behind the delaminated LCD (dLCD). The angular dimensions of this screen at a viewing distance of 1m were 31.0° (w) x 18.8° (h). An unmodified version of this screen (i.e. with the front polarizer *in situ*, and no blue filter in place) was used to measure conventional VEP and ERG responses to luminance-modulated checkerboard patterns.

Table 1: Characteristics of filters employed. Polarimetry was conducted at a working wavelength of 460nm, except for filter Or, which was conducted at 597nm. Polymer colour filters from Lee Filters Ltd, UK**.**

Filter	Description	Luminance (cd/m^2)		Polarimetry					Optics / spectrometry	Use/Rationale
		Greyscale		AoP		ΔAoP	DLP			
		000	255	000	255		000	255		
0	No filter in place	182.1	183.6	36.5	-53.1	89.6	0.98	0.98	'White' screen with peaks at 451, 542, 593 nm along a continuous spectrum from 410 – 750 nm	Control study
B	Blue-transmitting filter (#075, 'evening blue')	6.14	6.16	37.2	-51.5	88.7	1.00	0.98	Peak transmission of 440 – 460 nm, with zero transmission > 550nm	Provides optimum wavelength for PPP
LP:	Linear polarizer	1.6	141.0		-46.7			0.98	Neutral density polymer dichroic polariser	Reverts the dLCD into a conventional luminance-modulated display
Or	Blue-blocking filter (#105, 'orange')	71.8	72.7	39.6	-49.1	88.7	0.97	0.92	Transmission of 550 – 800+ nm; zero transmission < 500nm	Only wavelengths greater than action spectrum of PPP – provides confirmation of zero response to luminance artefacts
DP1	High-order (8^{th}) polymer linear retarder (retardation = 460 x 8 nm)	160.8	162.2	16.1	-78.0	94.1	0.29	0.30	Retardation axes set at 45° to resting polarisation state of screen	Scrambles the ellipticity and angle of incident polarisation for the waveband of the light source
DP2	High-order polymer linear retarder, as DP1	161.5	162	36.0	-50.8	86.8	1.00	0.99	Retardation axes aligned / perpendicular to resting screen polarisation.	Zero retardation effect at this angle, providing a control for DP1

Quantification of luminous intensity and polarization output (angle of polarization, AoP; degree of linear polarization, DLP) from each of the display screens was performed using a Minolta photometer (model CS100-A) and standard polarimetric methods, as described elsewhere (Foster et al., 2018; Misson & Anderson, 2017). For this purpose, the greyscale values 000 and 255 were quantified.

The polarimetry results for the control study display screen, for each individual filter and for no filter, are given in Table 1. Note that luminous intensity is independent of greyscale, except when the linear polarizer (LP) is *in situ*. The degree of polarization for all configurations was >90%, except for depolarizing filter 1 (DP1), where the DLP was approximately 30%. The difference in AoP between greyscale values was constant at approximately 90° for all settings, except for the pseudo-depolarizing high-order retarder (DP1) and linear polarizer (LP) settings. No polarization values are given for LP greyscale set to 000, as the luminous output for this configuration was less than 0.70 cd/m^2. Polarimetry was performed at 460 nm for all cases, except the blue-blocking filter (Or), where it was performed for the peak wavelength of 597 nm.

Similar polarimetry findings were found for the large polarization study display screen, where there was constant luminous output of 7.8 – 8.0 cd/m^2 that was independent of greyscale, and the difference in AoP between greyscales 000 and 255 was approximately 90°, with a constant DLP of 0.99. The unmodified large screen used for assessing luminance-modulated evoked responses had a constant AoP of 45° and a DLP of 1.00, and generated a high luminance difference between greyscale values of 000 (0.65 cd/m^2) and 255 (315.20 cd/m^2).

For both the small and large display screens, there is no recordable change in luminance switching between greyscales of 000 and 255 for viewing angles less than 30°. For the small screen, with a viewing distance of 25 cm and a large pupillary distance of 70 mm, the angle each eye makes with the screen is 8°. For the large screen viewed at 1 m, this angle reduces to 2°. Therefore, for both screens the maximum angle from perpendicular of gaze for each eye is well within the range where there are no detectable luminance effects.

2.2 Response recording

All VEP and ERG recordings were made with natural pupils in a dimly-lit room in accordance with the protocols published by the *International Federation of Clinical Neurophysiology* and the *International Society for the Clinical Electrophysiology of Vision* (Bach, Brigell, Hawlina, Holder, Johnson, McCulloch, Meigen & Viswanathan, 2013; Odom, Bach, Brigell, Holder, McCulloch, Mizota, Tormene & International Society for Clinical Electrophysiology, 2016). Participants were seated without head restraint, with their eyes level with a red fixation spot in the centre of the screen. Except where indicated, all results are for binocular viewing.

Both VEPs and ERGs were elicited by a checkerboard stimulus that contained equal numbers of black (greyscale = 000) and white (greyscale = 255) 1° checks, counterphased at 1.9 Hz. Participants fixated a 2 mm red spot at the centre of the field, where the corner of four checks met. A pictorial representation of the stimulus, with the blue-transmitting filter (#075, 'evening blue') in place, is shown in Figure 1a. Simulated percepts of the checkerboard, in different temporal phases, are shown in Figures 1b and 1c. The simulations, using methods detailed elsewhere (Misson et al., 2019), were generated assuming foveal viewing on the red fixation target at the geometric centre of the stimulus.

Recording sessions for all participants were completed over a period of four weeks, with each session lasting approximately 45 minutes. All recordings were made using the Micromed System PLUS/Evolution (Micromed, Mogliano Veneto, Italy). For VEP measures, the sampling rate was 4096 Hz, with potential differences amplified and band-passed filtered at 0.5—100 Hz. The VEP acquisition time-base was 500 ms, with 120 stimulus reversals averaged to obtain the response. For ERG measures, the sampling rate was 8192 Hz, with potential differences amplified and band-passed filtered at 1—100 Hz. The ERG

acquisition time-base was 200 ms, with the response averaged from 200 stimulus reversals. The rejection level for all recordings was set to ±30 μV, and response consistency was verified by a minimum of two similar waveforms for each test condition.

For VEP measures, silver-silver chloride disposable cup electrodes (from Spes Medica, Italy) were attached to the scalp – freshly cleaned with abrasive gel – using a combination of conductive paste and tape. Accepted electro-skin impedances were less than 5Ω. The electrodes were positioned as per the International 10/20 system (Odom, Bach et al., 2016), with active electrode Oz referred to Fz, O1 referred to Fz and O2 referred to Fz. A separate surface ground electrode was positioned on the forehead.

For ERG measures, DTL fibre electrodes (from Unimed Electrode Supplies Ltd, UK) were positioned, without topical anaesthetic, in close proximity to the upper margin of the lower eyelid. Fibre stability was achieved by taping the electrode near the nasal canthus. Surface reference electrodes were placed on the skin near the ipsilateral outer canthus of each eye. A surface ground electrode was positioned on the forehead.

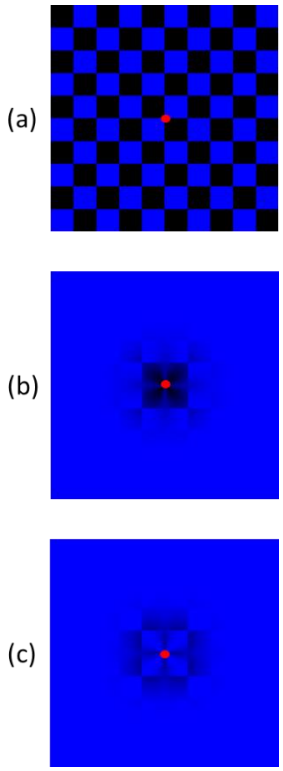

Figure 1: *Pictorial representation of the checkerboard stimulus with the blue-transmitting filter (#075 from Table 1) in place (a), and simulated percepts of the checkerboard in two different temporal phases (b and c). Simulations assumed foveal viewing on the red fixation target, and were completed using methods detailed elsewhere (Misson et al., 2019).*

2.3 Statistical analyses

For each participant, one-tailed paired-samples t-tests with α set at 0.05 using Bonferroni correction for multiple comparisons were conducted to assess the significance of post-stimulus deflections from baseline measures of noise.

2.4 Participants

Five individuals (age range 19—29 years; 1 male, 4 females) volunteered to participate. All were free from neurological and ocular disease, and all had full visual fields and normal or corrected-to-normal visual acuity. If required, a participant's refractive error was corrected using non-birefringent glass trial lenses. Informed consent was obtained from all participants. Experimental procedures were approved by the Aston University Research and Ethics Committee, and conformed to the tenets of the Declaration of Helsinki.

3. Results and Discussion

For both luminance- and polarization-modulated patterns, no laterality changes were evident in the VEP responses (i.e. the morphology of the Fz/O1 and Fz/O2 traces were near identical to that of the Fz/Oz trace). As such, all VEP traces reported below reflect the active electrode Oz referred to Fz.

3.1 Experiment 1: Preliminary and Control measures for VEP responses

Experiment 1 was designed to establish that a recordable response to a polarization pattern stimulus existed and that our protocol, employing the use of delaminated LCD screens for assessing polarization responses, did not produce any confounding luminance artefacts from either the display itself (see Odom et al., 2016) or from spurious stimulus generation. In completing these measures, we further determined the chromatic sensitivity of any evoked responses.

To define the normal luminance response for our control experimental setup, we first measured the standard pattern-reversal VEP for high contrast, achromatic, luminance-modulated checkerboard patterns. This was accomplished by placing filter 'LP' (from Table 1) into the exchangeable filter tray positioned at the front surface of the small monitor, which reverted the dLCD into a conventional luminance-modulated display. The results are shown in Figure 2 for one observer. Near identical results were obtained in two other observers. Note that the elicited response contains the signature N75, P100 and P135

components, typical of a VEP elicited by a luminance-modulated, pattern-reversal stimulus (see Odom et al., 2016).

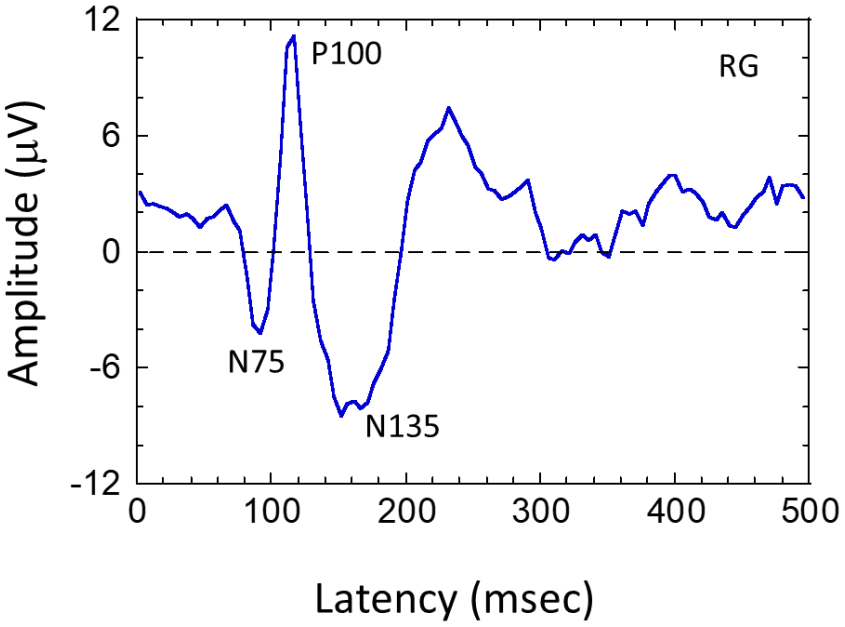

Figure 2: *Conventional pattern-reversal VEP for a high contrast, achromatic, luminance-modulated checkerboard pattern, for observer RG with binocular viewing. Measurements were completed using the small dLCD screen, with the 'LP filter (from Table 1) placed in the filter tray at the front surface of the monitor. The recorded trace, showing post-stimulus deflections N75, P100 and N135, reflects the active electrode Oz referred to Fz.*

The responses to a polarization pattern stimulus and the results of the control measures are shown in Figure 3 for three observers. Each row of panels (a – e) reflects the use of a given filter from Table 1. Positive (P) post-stimulus deflections from baseline are labelled a P_P1, where the subscript 'p' indicates a polarization response and the numeral indicates the order of response. The same classification system was used to denote observable negative (N) responses. The statistical significance of the deflections, determined for each observer using paired-samples t-tests (Bonferroni corrected for multiple comparisons), are reported in Table 2. All significant post-stimulus deflections are highlighted in Figure 3 using a conventional number of asterisks to denote different levels of significance (see figure caption for details). Non-significant deflections ($p > 0.05$) are labelled *ns*.

In Figure 3, rows (a) and (b) show the pattern-reversal polarization response (PolVEP) for blue and white linearly polarized light, respectively. Because macular pigment preferentially absorbs short wavelength light, it was assumed that the use of a blue coloured filter (with peak transmission of 440 – 460 nm) would elicit a stronger and/or more robust response than broad-spectrum white light. This assumption was confirmed, as the post-stimulus deflections from baseline in the elicited waveform with blue polarized light (P_P1, N_P1, N_P2) are generally of greater amplitude than those elicited with white polarized light [compare rows (a) and (b)]. Note, however, that the component amplitudes of polarization response with blue light are still less than those of the luminance VEP response with achromatic checkerboard patterns [compare row (a) for observer RG with Figure 2]. Row (c) shows the response elicited to polarized light that contains only wavelengths greater than 550 nm. Note the absence of any observable post-stimulus deflections in the waveform, consistent with reports that wavelengths greater than 550 nm fall outside the spectrum of those required for polarization pattern perception (Misson & Anderson, 2017). Row (d) shows the elicited response with a pseudo-depolarizing high-order retarding filter in place, which effectively scrambles both the ellipticity and angle of polarization of light reaching the eye over the waveband of polarization sensitivity. The absence of any response in row (d) provides confirmatory evidence that the elicited PolVEP shown in row (a) is due to light polarization, and was not the result of luminance or other artefacts in the display. This conclusion is reinforced by demonstrating the presence of a recordable PolVEP when the same high-order retarder is rotated by 45° to the polarization angles of the pattern stimulus [row (e)].

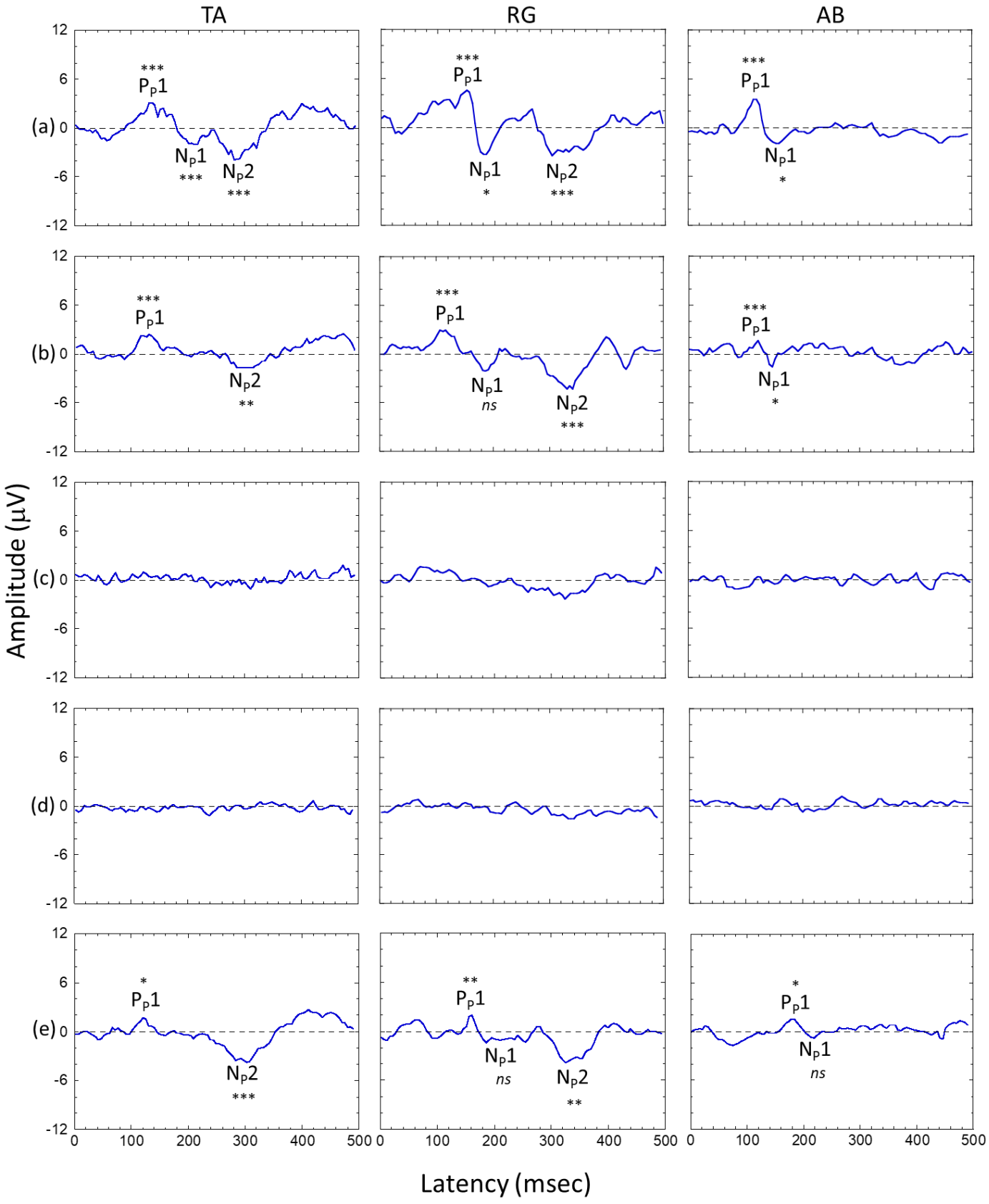

Figure 3: *Experiment 1 control measures for observers TA (left-hand panels), RG (middle panels) and AB (right-hand panels), completed with a 7-inch dLCD screen with an*

exchangeable filter tray positioned at the front surface of the monitor (see Methods for details). All VEP traces reflect the active electrode Oz referred to Fz, and all results are for binocular viewing. The various filters used were: (a) filter 'B', which produces an optimally coloured (i.e. blue) linearly polarized light for the human macular; (b) no filter, which produces white linearly polarized light; (c) filter 'Or', which only allows the transmission of wavelengths greater than the action spectrum of polarization pattern perception (i.e. > 550 nm; see Misson and Anderson, 2017); (d) pseudo-depolarizing filter DP1; and (e) filter DP2, which is DP1 rotated through 45°, thereby negating the depolarizing effect but maintaining free light transmission. See Table 1 for full details of filter characteristics. Observable positive and negative post-stimulus deflections from baseline are labelled (see text for details). The statistical significance of deflections are highlighted with asterisks (p< 0.05; ** p< 0.001; *** p< 0.001; ns indicates not significant). Details of statistical analyses, together with response latencies and amplitudes, are reported in Table 2.*

***Table 2**: Details of Experiment 1 control measures for observers TA, RG and AB, corresponding to the polarization VEP traces shown in Figure 3. For each observer, the latency (ms), amplitude (μV) and statistical significance of the post-stimulus deflections are shown for each filter type used (filters B, LB, Or, DP1 and DP2, as defined in Table 1). All results are for binocular viewing. All reported values reflect the active electrode Oz referred to Fz.*

		TA		RG		AB	
Filters (table 1)	**Deflection**	**Latency (ms)**	**Amplitude (μV)**	**Latency (ms)**	**Amplitude (μV)**	**Latency (ms)**	**Amplitude (μV)**
(A) B	P_p1	134.6	3.2 (t=5.1, p< .001)	150.9	4.6 (t=11.6, p< .001)	117.1	3.5 (t=6.1, p< .001)
	N_p1	207.9	-2.2 (t=-4.4, p< .001)	181.6	-3.4 (t=-2.5, p= .04)	157.5	-2.1 (t=-2.7, p= .03)
	N_p2	286.7	-4.1 (t=-8.6, p< .001)	319.5	-3.2 (t=-7.7, p< .001)		absent
(B) LB	P_p1	126.9	2.3 (t=4.6, p< .001)	111.6	2.9 (t=5.0, p< .001)	122.5	1.6 (t=4.8, p< .001)
	N_p1		absent	184.9	-2.2 (t=-1.4, p= .28)	145.5	-1.6 (t=-2.5, p= .04)
	N_p2	297.6	-1.8 (t=-3.4, p= .003)	332.6	-4.4 (t=-4.9, p< .001)		absent
(C) Or			no observed response		no observed response		no observed response
(D) DP1			no observed response		no observed response		no observed response
(E) DP2	P_p1	122.5	1.7 (t=2.4, p= .03)	158.6	1.9 (t=4.7, p= .002)	180.5	1.6 (t=2.8, p= .02)
	N_p1		absent	215.0	-1.2 (t=-1.0, p= .53)	216.6	-0.9 (t=-0.2, p= .86)
	N_p2	295.4	-3.8 (t=-6.3, p< .001)	332.6	-3.9 (t=-3.2, p= .006)		absent

3.2 Experiment 2: Polarization VEP and ERG responses

Having established that a VEP can be recorded to patterned stimuli defined solely by their polarisation **E**-vector orientation, we next used the same pattern-reversal protocol to quantify further the electrophysiological responses (VEP and PERG) to polarization stimuli.

As in our initial experiment, we first assessed whether our large screen experimental setup elicited conventional VEP and ERG waveforms to high-contrast, luminance-modulated checkerboard patterns. For this purpose, we used an unmodified version of our large polarization screen (i.e. with the front polarizer *in situ*, and no blue filter). The results are shown in Figure 4 for observer RG. Note that the elicited VEP waveform (top panel) is typical of that observed for normally sighted individuals, with a prominent P100 peak (amplitude 11.2 μV) sandwiched between the N75 and N135 components. Note also that, for observer RG, the VEP response measured using the large-screen display setup is comparable in both form and amplitude to that measured using the small-screen display setup [compare Figure 4 (top panel) with Figure 2]. The elicited ERG waveform (Figure 4, bottom panel) is also typical of that measured clinically, with a prominent P50 peak (of amplitude 6.1 μV) followed by a prominent N95 component (of amplitude 4.7 μV). Similar pattern-reversal response waveforms were found for all four participants who took part in the ERG trials.

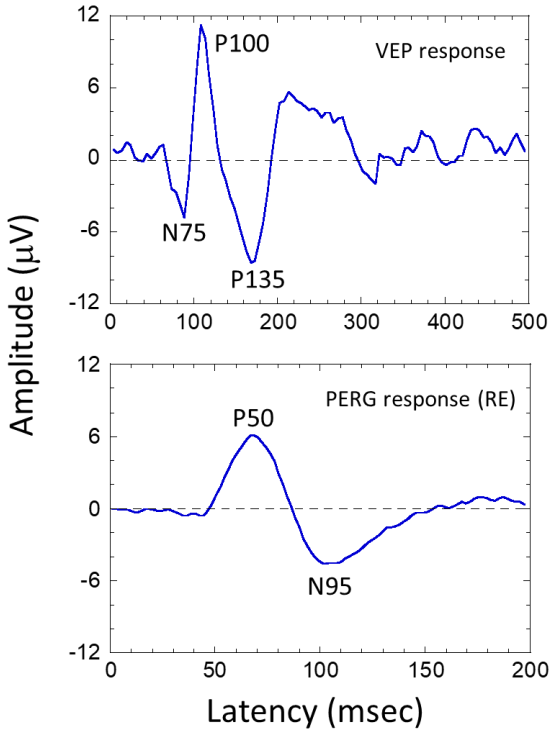

***Figure 4**. Standard VEP (binocular) and PERG (right eye) responses to high contrast (99.6%), counterphased (1.9 Hz), luminance-modulted checkerboard patterns obtained using the*

large-screen display setup (see Methods for details). The results are for observer RG. The VEP trace reflects the active electrode Oz referred to Fz.

3.2.1 Polarization-modulated VEP responses (PolVEP)

We next assessed the visual evoked potential to an isoluminant, isochromatic angle of polarization-modulated pattern, achieved by displaying the generated checkerboard patterns on the large delaminated screen that incorporated a blue-transmitting filter (see Methods and Table 1). Our principal goal in experiment 1 was to determine whether an electrophysiological response can be recorded to polarization stimuli, and for this purpose we employed binocular measures. Experiment 2 is a more detailed investigation of the polarization VEP response, and includes both monocular and binocular measures.

The results for five observers are shown in Figure 5, for monocular (left-hand panels) and binocular viewing (right-hand panels). Details of the latency (ms), amplitude (μV) and statistical significance of the post-stimulus PolVEP responses for all five participants are given in Table 3. Note that the elicited PolVEP waveforms are quantitatively and qualitatively distinct from that elicited by a clinically standard pattern-reversal protocol using high contrast achromatic luminance-modulated checks (compare Figures 4 and 5). For polarization-modulated patterns, for both monocular and binocular viewing, there was an initial prominent and significant ($p< 0.01$) peak at approximately 155 ms (termed P_P1) in all participants. This peak was followed by more variable (in terms of latency, amplitude and presence) negative deflections near 200 ms (N_P1) and 300 ms (N_P2). Significant post-stimulus deflections are highlighted in Figure 5 using asterisks to denote different levels of significance (see figure caption for details). Non-significant deflections ($p> 0.05$) are labelled *ns*. Note that, for each observer, there were no systematic latency or amplitude differences between the monocular and binocular responses.

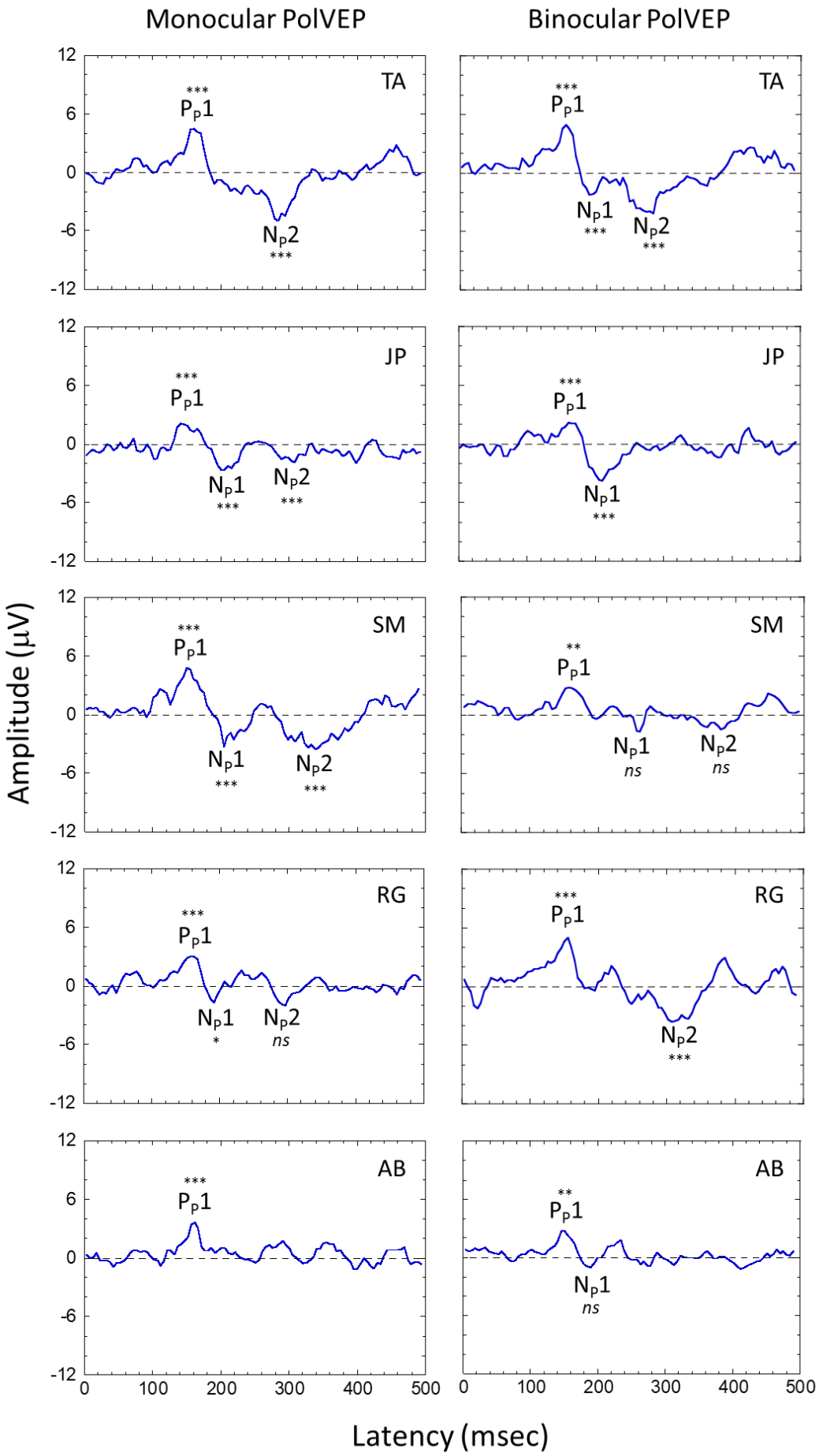
Monocular PolVEP
Binocular PolVEP
TA
JP
SM
RG
AB
PP1
NP1
NP2
***
**
*
ns
Amplitude (µV)
Latency (msec)
12
6
0
-6
-12
0
100
200
300
400
500

Figure 5: *Monocular (left-hand panels) and binocular (right-hand panels) polarization responses (PolVEP) for five participants, measured using the large-screen dLCD monitor. All traces reflect the active electrode Oz referred to Fz. The stimulus was an isoluminant, isochromatic polarization checkerboard pattern, counterphased at 1.9 Hz. Post-stimulus deflections from baseline are evident at latencies near 150 ms (P_P1), 200 ms (N_P1) and 300 ms (N_P2). The capital letters P and N refer to positive and negative deflections, respectively; the subscript 'p' is used to denote a polarization response. The statistical significance of the deflections are highlighted with asterisks (* p< 0.05; ** p< 0.001; *** p< 0.001; ns indicates not significant). Details of statistical analyses, together with response latencies and amplitudes, are reported in Table 3.*

***Table 3**: Details of Experiment 2 polarization measures for five observers, corresponding to the polarization VEP traces (PolVEP) shown in Figure 5. For each observer, the latency (ms), amplitude (μV) and statistical significance of the post-stimulus deflections (P_P1, N_P1, N_P2) are shown for both monocular (right eye, OD) and binocular viewing (OU). Values were averaged across participants to determine the mean latency (± 1 sem) and amplitude (± 1 sem) for each observable post-stimulus deflection. All reported values reflect the active electrode Oz referred to Fz.*

		P_P1		N_P1		N_P2	
Observer	**Eye**	**Latency (ms)**	**Amplitude (μV)**	**Latency (ms)**	**Amplitude (μV)**	**Latency (ms)**	**Amplitude (μV)**
TA	OD	157.5	4.4 (t=9.80, p<.001)	absent	absent	282.3	-4.9 (t=-13.55, p<.001)
	OU	155.4	4.9 (t=6.30, p<.001)	191.5	-2.3 (t=-7.49, p<.001)	272.5	-3.9 (t=-16.31, p<.001)
JP	OD	143.3	2.1 (t=4.55, p=.001)	204.6	-2.6 (t=-6.48, p<.001)	305.3	-1.9 (t=-6.45, p<.001)
	OU	161.9	2.1 (t=5.38, p<.001)	207.9	-3.8 (t=-7.01, p<.001)	absent	absent
SM	OD	152.1	4.8 (t=6.56, p<.001)	204.6	-3.5 (-6.77, p<.001)	339.2	-3.6 (t=-8.83, p<.001)
	OU	158.0	2.9 (t=3.83, p=.003)	260.0	-1.9 (t=-1.84, p=.15)	367.6	-1.2 (t=-0.71, p=.74)
RG	OD	158.6	3.0 (t=8.40, p<.001)	192.5	-1.9 (t=-2.84, p=.023)	296.5	-2.0 (t=-1.95, p=.12)
	OU	154.3	5.0 (t=7.47, p<.001)	absent	absent	308.5	-3.7 (t=-10.51, p<.001)
AB	OD	159.7	3.6 (t=6.53, p<.001)	absent	absent	absent	absent
	OU	148.8	2.9 (t=4.23, p=.002)	186.0	-1.2 (t=-0.79, p=.45)	absent	absent
$\bar{X} \pm 1$ **sem**	OD	154.2±3.0	3.6±0.5	200.6±4.0	-2.7±0.5	305.8±12.1	3.1±0.7
	OU	155.7±2.2	3.6±0.6	211.4±16.9	-2.3±0.6	316.2±27.7	-2.9±0.9

3.2.2 Polarization-modulated PERG responses

Using the same polarization stimuli employed to measure PolVEP responses, we attempted to measure an electroretinogram response using an otherwise standard clinical PERG protocol (see Methods). However, despite averaging up to 180 trials, no response was evident in any participant. There are at least four possible reasons why this should be so. First, stimuli confined to the macular alone are known to elicit a diminished response (Thompson & Drasdo, 1987; Drasdo, Cox & Thompson, 1987). Second, the low mean luminance of the delaminated display screen with the blue filter in place (approximately 6 cd/m^2) would make it difficult to elicit a PERG response (Bach et al., 2013). Third, although the computer-generated luminance contrast exceeded 99%, the maximum luminance contrast of the polarization pattern at the photoreceptor level (i.e. the luminance contrast after the polarization image had passed through the macular radial diattenuator) is an order of magnitude less (Misson & Anderson, 2017), again making it difficult to record a pattern ERG (Ben-Shlomo, Bach & Ofri, 2007). Finally, because the representation of retinal ganglion cells in the cortex is disproportionately larger for foveal midget cells than for ganglion cells elsewhere in the retina, signals arising from the macular are more detectable at the cortical level relative to the periphery.

4. General discussion and conclusion

Following subjective evidence that polarization-modulated patterns are identifiable across a range of contrasts and spatial scales (Misson and Anderson, 2017), we sought to determine whether an electrophysiological signature of human polarization perception could be identified. We did so in the belief that, because human polarization sensitivity is critically dependent on the anatomical integrity of the macula and the absorption properties of macular pigment (McGregor et al., 2014; Temple et al. 2015; Misson and Anderson, 2017), an objective measure of it may provide a unique means of assessing and monitoring macular function.

We demonstrated, for the first time, that a patterned stimulus modulated solely by difference in angle of linear polarization can elicit a visual evoked cortical response (Figure 5 and Table 3). Furthermore, we demonstrated that the response is due to linear polarization in the absence of luminance modulation, that the response is strongest in predominantly blue wavebands, and is absent when wavelengths less than 550 nm are excluded (i.e. wavebands corresponding to the absorption / transmission characteristics of macular pigment) (Figure 3 and Table 2). We therefore conclude that our results are the electrophysiological consequence of human polarization pattern sensitivity.

The only other electrophysiological study of polarized light sensitivity in humans is that of Dodt et al. (Dodt & Kuba, 1990; Dodt et al., 1994), who measured an onset/offset VEP response to Haidinger's brushes (a uniform linear polarization field stimulus). Although the

protocol and stimulus employed by Dodt et al. were too disparate to those used here to make any direct comparison, we do note that the dominant potentials he recorded were of long latency, as was the case in the present study, and that no electroretinographic response was recorded.

The initial positive deflection in the PolVEP (termed P_P1) was evident in all participants, peaking at approximately 150 ms (Figure 5). This compares with the initial positive deflection in a standard pattern-reversal VEP, termed the P100, which peaks at a latency near 100 ms (Odom et al., 2016). Conventional VEP recordings are typically completed using high luminance targets (> 100 cd/m^2), whereas our PolVEP measures, with the blue filter in place, were necessarily completed using low luminance targets (approximately 6 cd/m^2, Table 1).Therefore, the difference in latencies between polarization and conventional VEP responses may, in part, relate to the low luminance stimuli used in polarization measures, for it is known that conventional VEP latencies are delayed with dim targets (Drislane, 2007). It is also worth noting that our polarization responses reflect a pure macular response, and as such there was no contribution to the responses from peripheral retina, a state which is unlikely with conventional VEP recordings. It is known that the latency of conventional VEP responses varies with the extent to which the magnocellular pathway contributes to the evoked potential, with greater involvement leading to shorter latencies (Baseler and Sutter, 1997)

Clinical applications of polarization sensitivity, either to Haidinger's Brushes or to the more quantifiable polarization pattern perception, have been discussed elsewhere with respect to the diagnosis and monitoring of macular disease (Muller et al., 2016; Misson & Anderson, 2017), and the measurement of macular pigment density (Temple et al., 2019). Our findings that polarization stimuli also generate recordable visual evoked cortical responses extend the clinical application of human polarization perception to an objective test of macular function that does not rely on a conscious response. More specifically, we suggest that the following features are of practical use: (a) the initial positive deflection in the pattern-reversing polarization response (termed P_P1), which was a consistent and significant ($p< 0.01$) feature in all participants (Figure 5, Table 3); and (b) a blue stimulus corresponding to the absorption spectrum of macular pigment, which yields higher amplitude responses than broad-spectrum achromatic patterns (Figure 3). While the polarization response on its own may be insufficient to detect macular dysfunction, we suggest that it could form a valuable part of a suite of other diagnostic tests of central retinal function.

Macaque and other primates have similar macular architecture to humans (Bringmann, Syrbe, Görner, Kacza, Francke, Wiedemann & Reichenbach, 2018), and have been used as experimental models for human age-related macular degeneration (McGill, Renner & Neuringer, 2016). **E**-vector orientation-dependent foveal ganglion cell responses have been recorded in Macaques, and related to differential absorption by macular pigment (de

Monasterio, 1978). While the existence of polarization-modulated visual evoked responses in these species is yet to be reported, if present, such responses could be a useful objective measure of macular function and the assessment of pharmacological interventions in the treatment of macular disease.

Acknowledgements:
We thank Prof. Paul Furlong for general advice on electrophysiological recordings, and the administrative staff at the Aston Neuroscience Institute.

Author contributions
SJA methodology, data collection and analysis, writing original draft, review and editing.
AE-S methodology, data collection and analysis, review and editing, project administration.
GPM conceptualization, methodology, data collection and analysis, writing original draft, review and editing.

References

Bach, M., Brigell, M.G., Hawlina, M., Holder, G.E., Johnson, M.A., McCulloch, D.L., Meigen, T., & Viswanathan, S. (2013). ISCEV standard for clinical pattern electroretinography (PERG): 2012 update. *Doc Ophthalmol, 126* (1), 1-7.

Baseler, H.A. & Sutter, E.E. (1997). M and P components of the VEP sn their visual field distribution. *Vision Res*, 37, 675-690.

Ben-Shlomo, G., Bach, M., & Ofri, R. (2007). Temporal and spatial frequencies interact in the contrast transfer function of the pattern electroretinogram. *Vision Res, 47* (15), 1992-1999.

Bringmann, A., Syrbe, S., Görner, K., Kacza, J., Francke, M., Wiedemann, P., & Reichenbach, A. (2018). The primate fovea: Structure, function and development. *Progress in Retinal and Eye Research, 66*, 49-84.

de Monasterio, F.M. (1978). Macular pigmentation and spectral sensitivity of retinal ganglion cells of macaques. *Vision Research, 18* (10), 1273-1277.

Dodt, E., & Kuba, M. (1990). Visually evoked potentials in response to rotating plane-polarized blue light. *Ophthalmic Res, 22* (6), 391-394.

Dodt, E., Tsuyama, Y., & Kuba, M. (1994). [Sensory and electrical responses in stimulation of the macula with short-wave (407-527 nm) linear polarized light (Haidinger polarization brushes)]. *Ophthalmologe, 91* (2), 169-175.

Drasdo, N., Cox, W., & Thompson, D.A. (1987). The effects of image degradation on retinal illuminance and pattern responses to checkerboard stimuli. *Doc Ophthalmol, 66* (3), 267-275.

Drislane, F.W. (2007). Visual Evoked Potentials. In A.S. Blum & S.B. Rutkove (Eds) *The Clinical Neurophysiology Primer* (pp 461-473). Humana Press, New Jersey.

Foster, J.J., Temple, S.E., How, M.J., Daly, I.M., Sharkey, C.R., Wilby, D., & Roberts, N.W. (2018). Polarisation vision: overcoming challenges of working with a property of light we barely see. *Naturwissenschaften, 105* (3-4), 27.

Goldschmidt, M. (1950). A new test for function of the macula lutea. *Archives of Ophthalmology, 44* (1), 129-135.

Horváth, G. (2014). Polarized Light and Polarization Vision in Animal Sciences. (Springer.

McGill, T.J., Renner, L.M., & Neuringer, M. (2016). Elevated Fundus Autofluorescence in Monkeys Deficient in Lutein, Zeaxanthin, and Omega-3 Fatty Acids. *Investigative Ophthalmology & Visual Science, 57* (3), 1361-1369.

McGregor, J., Temple, S.E., & Horváth, G. (2014). Human Polarization Sensitivity. In: G. Horváth (Ed.) *Polarized Light and Polarization Vision in Animal Sciences* (pp. 303 - 315). Heidelberg: Springer.

Misson, G.P., & Anderson, S.J. (2017). The spectral, spatial and contrast sensitivity of human polarization pattern perception. *Scientific Reports, 7* (1), 16571.

Misson, G.P., Temple, S.E., & Anderson, S.J. (2019). Computational simulation of human perception of spatially dependent patterns modulated by degree and angle of linear polarization. *J Opt Soc Am A, 36* (4), B65-B70.

Misson, G.P., Timmerman, B.H., & Bryanston-Cross, P.J. (2015). Human perception of visual stimuli modulated by direction of linear polarization. *Vision Res, 115, Part A*, 48-57.

Muller, P.L., Muller, S., Gliem, M., Kupper, K., Holz, F.G., Harmening, W.M., & Charbel Issa, P. (2016). Perception of Haidinger Brushes in Macular Disease Depends on Macular Pigment Density and Visual Acuity. *Invest Ophthalmol Vis Sci, 57* (3), 1448-1456.

Odom, J.V., Bach, M., Brigell, M., Holder, G.E., McCulloch, D.L., Mizota, A., Tormene, A.P., & International Society for Clinical Electrophysiology of, V. (2016). ISCEV standard for clinical visual evoked potentials: (2016 update). *Doc Ophthalmol, 133* (1), 1-9.

Stanworth, A., & Naylor, E.J. (1955). The measurement and clinical significance of the Haidinger effect. *Trans Ophth Soc U.K., 75*, 67-79.

Temple, S.E., McGregor, J.E., Miles, C., Graham, L., Miller, J., Buck, J., Scott-Samuel, N.E., & Roberts, N.W. (2015). Perceiving polarization with the naked eye: characterization of human polarization sensitivity. *Proc. R. Soc. B, 282* (1811), 20150338.

Temple, S.E., Roberts, N.W., & Misson, G.P. (2019). Haidinger's brushes elicited at varying degrees of polarization rapidly and easily assesses total macular pigmentation. *J Opt Soc Am A, 36* (4), B123-B131.

Thompson, D.A., & Drasdo, N. (1987). Computation of the luminance and pattern components of the bar pattern electroretinogram. *Doc Ophthalmol, 66* (3), 233-244.